Biomedical Optics EXPRESS

Estimation of vessel diameter and blood flow dynamics from laser speckle images

Dmitry D. Postnov,[1,*] Valery V. Tuchin,[2,3,4] and Olga Sosnovtseva[1]

[1]*Department of Biomedical Sciences, Copenhagen University, Blegdamsvej 3, 2200 Copenhagen N, Denmark*
[2]*Research-Educational Institute of Optics and Biophotonics, Saratov National Research State University, Astrakhanskaya Str. 83,410012 Saratov, Russia*
[3]*Institute of Precision Mechanics and Control RAS, Rabochaya str. 24, 410028 Saratov, Russia*
[4]*Interdisciplinary Laboratory of Biophotonics, Tomsk National Research State University, 634050 Tomsk, Russia*
[*]*dpostnov@sund.ku.dk*

Abstract: Laser speckle imaging is a rapidly developing method to study changes of blood velocity in the vascular networks. However, to assess blood flow and vascular responses it is crucial to measure vessel diameter in addition to blood velocity dynamics. We suggest an algorithm that allows for dynamical masking of a vessel position and measurements of it's diameter from laser speckle images. This approach demonstrates high reliability and stability.

OCIS codes: (120.6150) Speckle imaging; (170.1470) Blood or tissue constituent monitoring; (170.5380) Physiology.

References and links

1. Y. Aizu and T. Asakura, "Bio-speckle phenomena and their application to the evaluation of blood flow," Opt. Laser Technol. **23**, 205–219 (1991).
2. D.A. Boas and A.K. Dunn, "Laser speckle contrast imaging in biomedical optics," J. Biomed. Opt. **15**, 011109 (2010).
3. D. Briers, D.D. Duncan, E. Hirst, and S.J. Kirkpatrick, "Laser speckle contrast imaging: theoretical and practical limitations," J. Biomed. Opt. **18**, 066018 (2013).
4. I.V. Fedosov and V.V. Tuchin, "Bioflow Measuring: Laser Doppler and Speckle Techniques," in *Coherent-Domain Optical Methods: Biomedical Diagnostics, Environmental Monitoring and Material Science*, 2nd ed. (Springer-Verlag, 2013) pp. 487–564.
5. H. Cheng, Y. Yan, and T.Q. Duong, "Temporal statistical analysis of laser speckle images and its application to retinal blood-flow imaging," Opt. Express **16**, 10214–10219 (2008).
6. C. Ayata, A.K. Dunn, Y. Gursoy-zdemir, Z. Huang, D.A. Boas, and M.A. Moskowitz, "Laser speckle flowmetry for the study of cerebrovascular physiology in normal and ischemic mouse cortex," J. Cereb. Blood Flow Metab. **24**, 744–755 (2004).
7. N.H. Holstein-Rathlou, O.V. Sosnovtseva, A.N. Pavlov, W.A. Cupples, and C.M. Sorensen, "Nephron blood flow dynamics measured by laser speckle contrast imaging," Am. J Physiol. Renal Physiol **300**, F319–F329 (2011).
8. D.D. Postnov, N.-H. Holstein-Rathlou, and O. Sosnovtseva, "Laser speckle imaging of intra organ drug distribution," Biomed. Opt. Express **6**, 5055–5062 (2015).
9. G. Mahe, A. Humeau-Heurtier, S. Durand, G. Leftheriotis, and P. Abraham, "Assessment of skin microvascular function and dysfunction with laser speckle contrast imaging," Circulation: Cardiovascular Imaging **5**, 155–163 (2012).
10. D. Chen, J. Ren, Y. Wang, H. Zhao, B. Li, and Y. Gu, "Relationship between the blood perfusion values determined by laser speckle imaging and laser Doppler imaging in normal skin and port wine stains," Photodiagnosis Photodynamic Therapy **13**, 1–9 (2016).
11. A.J. Strong, E.L. Bezzina, P.J. Anderson, M.G. Boutelle, S.E. Hopwood, and A.K. Dunn, "Evaluation of laser speckle flowmetry for imaging cortical perfusion in experimental stroke studies: quantitation of perfusion and detection of peri-infarct depolarisations," J. Cereb. Blood Flow Metab. **26**, 645–653 (2006).

#264873 Received 9 May 2016; revised 10 Jun 2016; accepted 16 Jun 2016; published 22 Jun 2016

12. H. Nilsson and C. Aalkjaer, "Vasomotion: mechanisms and physiological importance," Molecular Interventions **3**, 79 (2003).
13. D.D. Postnov, O. Sosnovtseva, and V.V. Tuchin, "Improved detectability of microcirculatory dynamics by laser speckle flowmetry," J. Biophoton. **8**, 790–794 (2015).
14. Q. Liu, Y. Li, H. Lu, and S. Tong, "Real-time high resolution laser speckle imaging of cerebral vascular changes in a rodent photothrombosis model," Biomed. Opt. Express **5**, 1483–1493 (2014).
15. S.S. Kazmi, E. Faraji, M.A. Davis, Y.Y. Huang, X.J. Zhang, and A.K. Dunn, "Flux or speed? Examining speckle contrast imaging of vascular flows," Biomed. Opt. Express **6**, 2588–2608 (2015).
16. A.Y. Neganova, D.D. Postnov, J.C. Brings-Jacobsen, and O Sosnovtseva, "Laser speckle analysis of retinal vascular dynamics," Biomed. Opt. Express **7**, 1375–1384 (2016).

1. Introduction

Laser speckle imaging (LSI) offers full-field monitoring of relative blood flow with high temporal and spatial resolution [1–4]. Although many complex nonlinear processes are involved, laser speckle imaging is highly correlated with the velocity of red blood cells [5] and is often used to estimate flow dynamics [5–7]. However, the estimation of flow dynamics from the velocity is valid only when the vessel diameter remains constant. This is a case of study in microvascular networks of the kidney [7, 8], skin [9, 10] and brain capillaries [11]. Otherwise alterations of the diameter contribute significantly to flow changes. This challenges the evaluation of dynamical and vascular responses under spontaneous and induced vasomotion [12]. It is possible to achieve high quality diameter measurements with intermittent green light but this would lead to significant decline in temporal resolution and increased complexity of optical setup. Thus, it is important to estimate diameter dynamics directly from laser speckle data. Although attempts to estimate stationary vessel diameter from laser speckle data are known [14], dynamical changes of the diameter due to vasomotion were not discussed yet in the context of laser speckle imaging. We propose a computationally simple algorithm with fewer number of input parameters that allows for dynamical evaluation of vessel diameter from laser speckle data. The approach is based on the dynamical mask of vessels rather than on a choice of an appropriate region of interest and translates relative changes of blood velocity into relative dynamics of blood flow. The algorithm is oriented towards biomedical researchers.

2. Methods

All animal experimental protocols were approved by the Danish National Animal Experiments Inspectorate and were conducted in accordance with guidelines of the American Physiological Society. Coherent infrared light was delivered to the object from the laser module LDM785 controlled by diode driver Thorlabs CLD1011LP with the laser power density of about 10 mW/cm^2 [13]. The signal was collected by CMOS camera Basler acA2000-165umNIR with the exposure time of 5 ms while the field of view and frame rate were adjusted depending on the object. Several laser speckle experiments were performed: (i) *in vivo* experiments on a single artery with the diameter of 200 μm from rat mesenterium were designed to test the algorithm. The experiments were carried out on anesthetized rats with abdomen opened and messenterium exposed. A specially designed chamber with the volume of 300 μl filled with the sodium chloride solution was inserted under the messenterium. Mesenteric tissue was carefully dissected away from an artery and the vessel was fixed in the chamber. After baseline recording, a contractile response of the vessel was provoked by the administration of norepinephrine (NE) followed by the vasodilator acetylcholine (ACh). Pharmacological administration was carried by replacing 10% of physiological solution in the chamber with the corresponding drug; (ii) *in vivo* experiments of mouse cortex were designed to test the algorithm in combination with a vessel segmentation approach. Laser speckle recordings were performed through the scull during control and during short perfusion with NaCl. The scull was cannulated with two catheters: one

#264873 Received 9 May 2016; revised 10 Jun 2016; accepted 16 Jun 2016; published 22 Jun 2016

was for NaCl infusion and the other was for excess removal. Perfusion of the brain with NaCl led to a significant increase of vessel resistance and drop of blood velocity and flow. Schematic presentation of both experiment setups is given in Fig. 1.

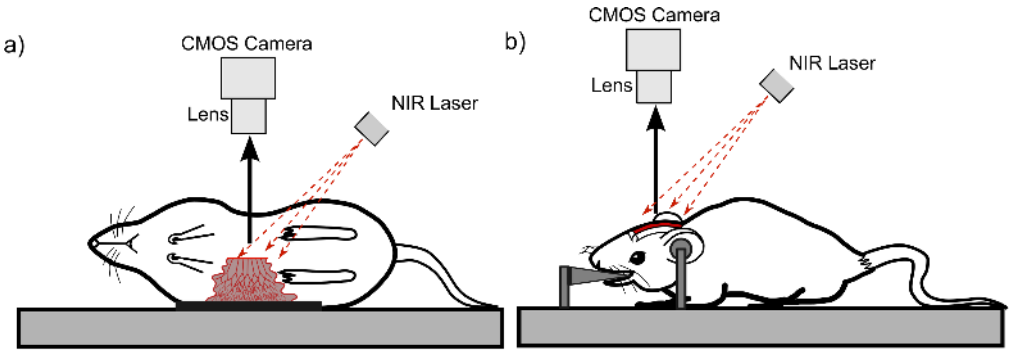

Fig. 1. Schematic presentation of the experiment setup: (a) Imaging of mesenterium arteries and (b) laser speckle imaging of vascular network in mouse cortex. Both experiments are done *in vivo* on anesthetized animals.

Since the present study covers the case when the vessel diameter is not constant, we use different terminology: "Speckle value (*SV*)" instead of "Blood flow index (*BFI*)". Speckle value is calculated in the same way as *BFI* introduced for the case of the constant vessel diameter. *SV* is proportional to the mean velocity of scattering particles [5]:

$$SV = \bar{I}^2/\sigma^2, \tag{1}$$

where $\bar{I}$ and σ are the mean value and the standard deviation of speckle intensity, calculated over 25 frames for each pixel.

Since speckle patterns recorded from a single *SV* frame are noisy, a precise estimation of the vessel diameter would require data smoothing. However, spatial smoothing leads to a significant error in the estimated diameter while temporal smoothing diminishes important dynamical variations of the diameter and enhances sensitivity to movements. In order to provide precise and robust diameter measurements we suggest an algorithm that builds a dynamical mask of the vessel and estimates changes in the diameter. The main features of the algorithm can be outlined as follows:

- **Input:** *LSIData* are *SV* values in 3D format (x, y, time). D_{min} is a minimal expected diameter of the vessel in pixels (default 1). *Error* is a maximal allowed relative error in the first mask estimation (default 100%). N is a number of consequential frames for temporal smoothing (default 3). Such set of parameters allows one to use the algorithm without heavy optimization. D_{min} can be estimated from LSI data by eye. N is set in accordance with expected dynamics and sampling rate. Although *Error* is set to 100% by default it can be reduced in the case if several pronounced vessels are located close to each other;
- **Output:** Dynamical binary mask of the vessel together with its diameter, vessel profile, *SV* values and flow dynamics;
- **Region requirements:** For reliable diameter estimation the vessel length in the region should be larger than the vessel width. In the case of vessel intersection or 90 degree

#264873 Received 9 May 2016; revised 10 Jun 2016; accepted 16 Jun 2016; published 22 Jun 2016

curvature, the vessels should not be parallel to the region borders. The vessel is assumed to have the same diameter within the region;

- **Tortuosity:** The algorithm is able to detect and follow tortuosity of the vessel as long as the above region requirements are met;
- **Movement robustness:** The algorithm is robust to vessel movements as long as the above region requirements are met and the initial vessel remains the most pronounced vessel in the region;
- **Precision:** The resulting error in diameter measurements depends on the quality of laser speckle images.

The algorithm is developed to detect dynamical changes in the vessel diameter. But it can be used in stationary state as well, although the averaged image provides efficient estimation of the diameter in this case.

Step-by-step description of the algorithm is presented in table 1 and Fig. 2.

#264873 Received 9 May 2016; revised 10 Jun 2016; accepted 16 Jun 2016; published 22 Jun 2016

Table 1. Algorithm description.

Action	Description	Input and output
Step I		
1. Temporal smoothing	Pixel by pixel moving average over all frames in *LSIData* with a smoothing kernel of *N* frames	**Input:** $LSIData(x,y,t)$,N **Output:** $SData1(x,y,t)$
2. Spatial smoothing	Gaussian filtering with standard deviation of $0.25D_{min}$	**Input:** D_{min}, $SData1(x,y,t)$ **Output:** $SData2(x,y,t)$
3. Horizontal masking (Fig. 2, step I, right)	Masking of the highest *SV* peak in each frame for each y value, while scanning in x direction	**Input:** $SData2(x,y,t)$ **Output:** $HMask(x,y,t)$
4. Vertical masking (Fig. 2 step I, left)	Masking of the highest peak *SV* in each frame for each x value, while scanning in y direction	**Input:** $SData2(x,y,t)$ **Output:** $VMask(x,y,t)$
5. Choice of the optimal direction (horizontal in Fig. 2)	Finding if the largest interconnected object is in $HMask(x,y,t)$ or in $VMask(x,y,t)$	**Input:** $HMask(x,y,t)$, $VMask(x,y,t)$ **Output:** $Mask1(x,y,t)$, $Direction$ (H or V)
6. Artifact removal	All interconnected objects except the largest one are removed	**Input:** $Mask1(x,y,t)$ **Output:** $Mask2(x,y,t)$
Step II		
7. Center line estimation (Fig. 2 step II, left)	Finding of the center of the masked region in the chosen direction for each frame	**Input:** $Mask2(x,y,t)$, Direction **Output:** $CMask1(x,y,t)$
8. Center line correction	Solitary peaks along the scan line are removed. The center line is smoothed with moving average with a kernel of D_{min} points.	**Input:** $CMask1(x,t)$ **Output:** $CMask2(x,y,t)$
9. Vessel profile estimation (Fig. 2, step II, right)	The angle of the center line is calculated. Vessel profile is calculated for each frame as an average of scan lines in the chosen direction and is centered along the center line $CMask2(x,y,t)$.	**Input:** $LSIData$, $CMask2(x,t)$ **Output:** $Profile(x,t)$, $Angle(t)$
Step III		
10. Border and diameter estimation (Fig. 2, step III)	Tracking of the minimum of the second order gradient of the vessel profile on both sides of the central line within the range $Mask2(x,y,t) \pm Error$	**Input:** $Profile(x,t)$, $CMask2(x,t)$, $Mask2(x,y,t)$ **Output:** $D(t)$, $Mask3(x,y,t)$
11. Center line estimation	The center of the masked region in the chosen direction is found for each frame and then smoothed by moving average.	**Input:** $Mask3(x,y,t)$ **Output:** $CMask3(x,y,t)$
12. Additional calculations	Estimating of the flow dynamics (FD) and velocity (SV) changes.	**Input:** $LSIData(x,y,t)$, $Mask3(x,y,t)$, $CMask3(x,y,t)$, $D(t)$ **Output:** SV_{line}, SV_{vessel}, FD_{line}, FD_{vessel}

#264873 Received 9 May 2016; revised 10 Jun 2016; accepted 16 Jun 2016; published 22 Jun 2016

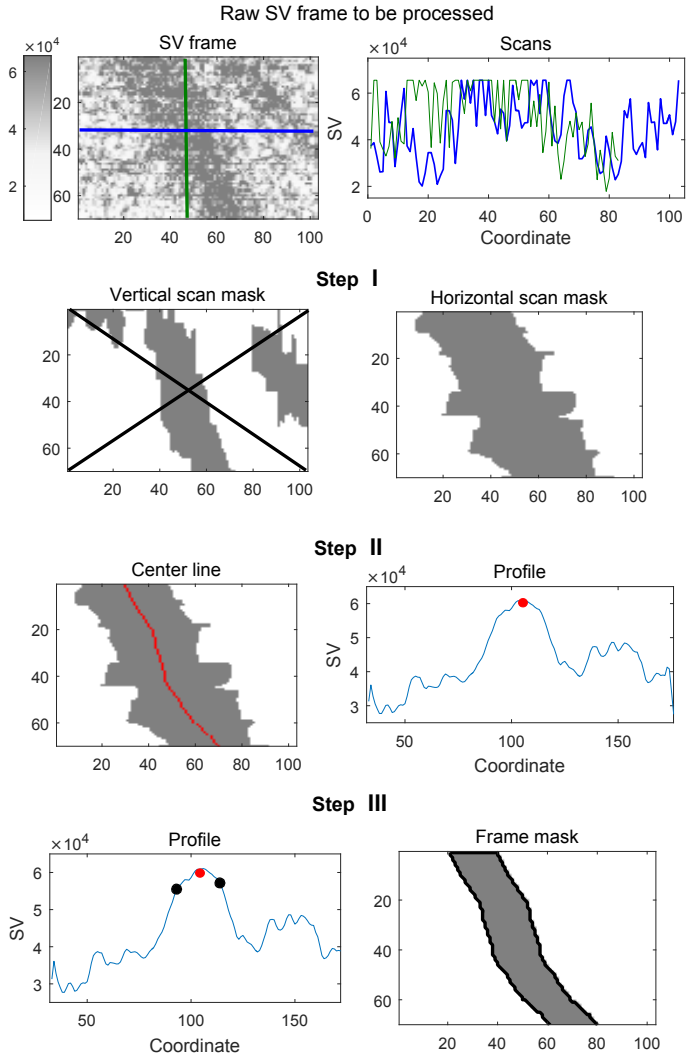

Fig. 2. Main steps of the algorithm for diameter estimation. The top panel represents a frame of non-smoothed laser speckle data and corresponding *SV* values along vertical (green) and horizontal (blue) scan lines. **Step I:** Rough estimation of the vessel location and geometry from smoothed data. Notice that the horizontal scan provides better visualization of the vessel geometry. **Step II:** Detection of the center line (red) that always belongs to the vessel, creation of the vessel profile obtained as an average of speckle values over all horizontal scan lines of the frame and centered along the center line coordinates. **Step III:** Estimation of the vessel boundary (black) by calculating a relative *SV* drop from the center line and the minimum of the second order gradient.

Although we used the second order gradient analysis at 3, 4, and 10 items of the table, one can use parabolic fitting in two scanning directions (e.g, see Ref. [14]) or any other vessel recognition approach. The user benefits the most from the developed algorithm when the diameter or vessel position changes in time.

#264873 Received 9 May 2016; revised 10 Jun 2016; accepted 16 Jun 2016; published 22 Jun 2016

3. Results

To estimate precision of the computed diameter we calculate a relative error as:

$$Error = \left| \frac{D_v - D_c}{D_c} \right| \times 100\%, \tag{2}$$

where D_v is a visually determined inner diameter measured by a specialist in three different places of the vessel and then averaged. D_c is a computationally estimated diameter. D_c represents either the diameter estimated from smoothed data using the second order gradient analysis (after Step I) or from the averaged vessel profile using the second order gradient analysis (item 10 in Step III). Figure 3 shows that the step III of the algorithm provides significantly higher precision in diameter measurements compared to the measurements at the step I. Notice that the error decreases with the increase of vessel diameter to be estimated.

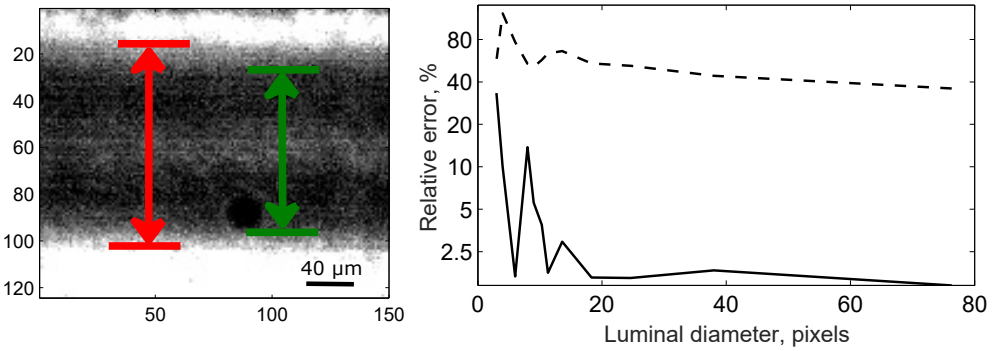

Fig. 3. Left panel: Microphotography of a vessel. Red color indicates the outer diameter and green color marks the inner diameter. Right panel: Relative error of the diameter estimation calculated from (2) after the step I (dashed curve) and for the step III (solid curve).

In addition to diameter measurements it is also important to understand what *SV* value stands for. Theory says it is proportional to the mean particle velocity [5, 6] or linked to it via complicated relations [15] while experimental circulation research often refers to it as a measure of blood flow [6, 7]. As we discussed, velocity is measured at all situations while blood flow measurements require additional information about the diameter (whether it is constant or changing). *SV* time courses are rarely calculated from a single pixel, typically they are averaged over a selected region of interest. When the diameter is not constant, *SV* dynamics depends on the size and position of regions of interest. This is related to changing number of pixels that belong to the vessel as the result of changing vessel diameter. As a consequence, this affects both velocity and flow dynamics.

#264873 Received 9 May 2016; revised 10 Jun 2016; accepted 16 Jun 2016; published 22 Jun 2016

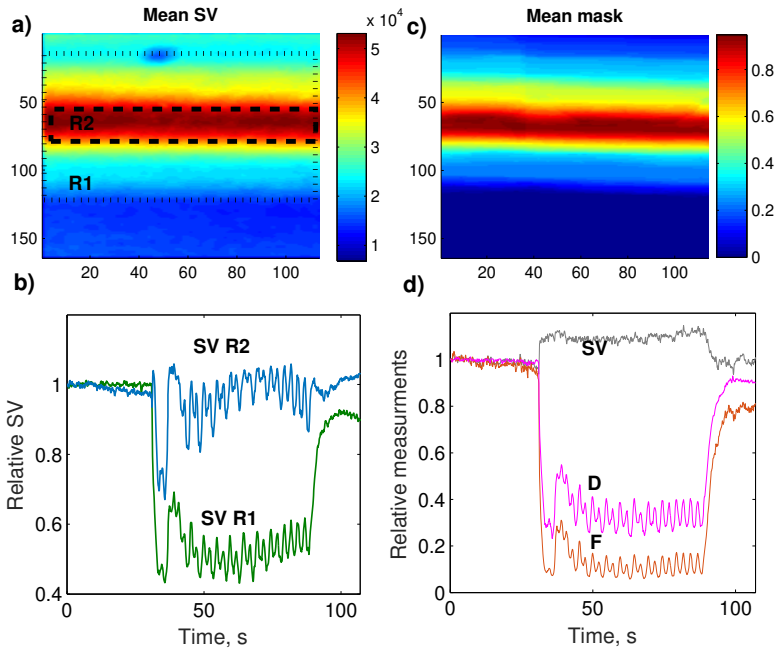

Fig. 4. Estimation of speckle value *SV* through the average over the regions of interest (left panels) and through dynamical masking approach (right panels). (a) *SV* frame averaged over 110 s. Regions R1 and R2 are chosen for the calculation of *SV*; (b) *SV* dynamics in R1 (green) and R2 (blue). Notice that dynamics depends significantly on the selected regions of interest; (c) Mask averaged over time. The higher values indicate that the vessel is detected at the corresponding pixels for longer time; (d) *SV* measured from the central line along the vessel (gray), diameter *D* calculated according to our algorithm (magenta) and flow dynamics *F* estimated from *SV* measurements and calculated diameter. All curves are normalized by the baseline value recorded for the first 10 s. Notice that *SV* dynamics calculated from the regions R1 and R2 does not correspond to the dynamics measured via dynamical masking. This difference is caused by changing diameter.

Such situation is illustrated in Fig. 4 where pharmacological stimulation provokes contractile response of the vessel followed by rhythmic oscillations of its diameter. One can see that *SV* time series recorded from two regions of interest R1 and R2 demonstrate different dynamics (a,b) compared to *SV* recorded along the center line of the dynamically masked region (c,d). Dynamical masking and *SV* measurements along the center of the vessel reveal that actual *SV* increases during vessel constriction. This is expected reaction of the blood velocity to local constriction of the vessel as depicted in Fig. 4(d). Knowing *SV* and diameter one can estimate blood flow dynamics in the vessel. Flow dynamics is calculated as:

$$F(t) = D(t)^2 \times SV(t), \tag{3}$$

where $D(t)$ and $SV(t)$ are diameter and speckle value at the moment of time t. Since we are interested in relative dynamical changes, constant coefficients can be neglected.

Another important application of the algorithm for vessel recognition and diameter estimation is a mapping of vascular responses not only in a single vessel but in intact network. In

#264873 Received 9 May 2016; revised 10 Jun 2016; accepted 16 Jun 2016; published 22 Jun 2016

this context, laser speckle imaging being a full-field method with relatively high spatial resolution provides the most benefit. A preliminary version of our algorithm was used to address the question: How do vessels of different diameters in the retinal network respond to stimuli [16]. Here, we demonstrate a possibility of using the algorithm for segmentation of vascular network images in accordance with vascular response of particular vessels. We measure diameter, *SV*, and flow dynamics over multiple vessels in the mouse cortex in the control and during perfusion of NaCl and visualize changes across the network (Fig. 5). Inspection of the figure shows how the diameter of network vessels drops at the beginning of the infusion and returns back to control values after adaptation period of continuous infusion. Using dynamical masking also ensures stability of the results with respect to small movements of the tissue while standard pixel-by-pixel algorithms can lead to significant artifacts. All together this allows one to study single vessel response to local stimuli *in vivo* and to detect propagation of the response along the vascular network.

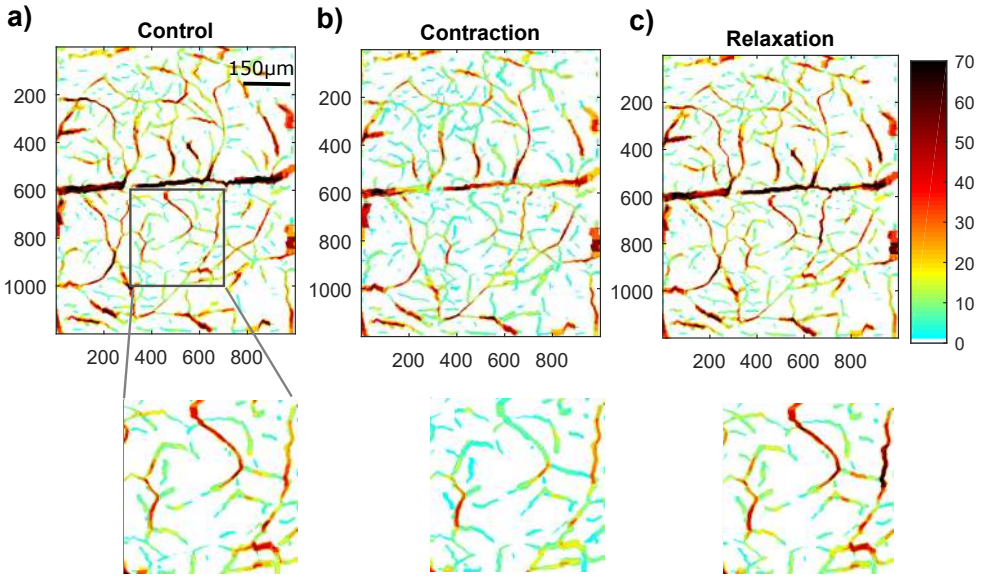

Fig. 5. Diameter changes in the mouse cortex vascular network during control measurements (a), vessel contraction at the beginning of NaCl perfusion (b), and vessel relaxation during continuous NaCl perfusion (c). The bottom panel shows the enlarged region marked on (a) for all three images on the top panel. Diameter of the vessels is coded by color. Color-coded diameter is mapped on the mask of vascular network. We used the same mask in (a), (b), and (c) that was calculated as an average mask over all frames.

4. Conclusion

In conclusion, we developed the algorithm for dynamical masking of vessels and measurements of their diameter from laser speckle data. With measured diameter and relative changes in erythrocyte velocity we are able to estimate blood flow dynamics that opens new perspectives for using LSI in vascular research. We also demonstrated that dynamical masking provides highly reliable results in the case of vasomotion in comparison with the results obtained from

#264873 Received 9 May 2016; revised 10 Jun 2016; accepted 16 Jun 2016; published 22 Jun 2016

fixed regions of interest. We showed that the algorithm can be used as a basis for segmentation process of laser speckle images and can be further applied to create different response maps. In this work we followed the assumption that the mean velocity of particles contributed the most into the formation of speckle images. It is known, however, that this dependency is nonlinear and is affected by particle density [15]. As for now, it is not possible to separate velocity and density components from laser speckle data. However, if one could separate contribution of each component (i.e. velocity, density, diameter) this would give an access to pressure variations in vascular beds that is not amenable by other methods yet.

Acknowledgments

Authors are thankful to Christian Aalkjær and Vladimir Matchkov for assistance with designing animal experiments and to Anastasiia Neganova for helping with figure design. V.V. Tuchin was supported by RFBR grant 14-02-00526, grant 14.Z50.31.0004 of the Russian Federation Government, and The Tomsk State University Academic D.I. Mendeleev Fund Program.

#264873 Received 9 May 2016; revised 10 Jun 2016; accepted 16 Jun 2016; published 22 Jun 2016